ELSEVIER

Journal of Alloys and Compounds 388 (2005) 235–240

Journal of ALLOYS AND COMPOUNDS

www.elsevier.com/locate/jallcom

Characterization of the microstructure of gas-atomized Nd–Fe–B alloy particles of non-peritectic chemical compositions

J. Gao[a,c,*], T. Volkmann[a], S. Reutzel[b], D.M. Herlach[a]

[a] *Institute of Space Simulation, German Aerospace Center, 51147 Cologne, Germany*
[b] *Institute of Experimental Physics IV, Ruhr-University of Bochum, 44780 Bochum, Germany*
[c] *Key Lab of Electromagnetic Processing of Materials, Northeastern University, Shenyang 110004, China*

Received 14 June 2004; received in revised form 6 July 2004; accepted 6 July 2004

Abstract

Gas-atomized Nd–Fe–B droplets of non-peritectic chemical compositions $Nd_{16}Fe_{76}B_8$, $Nd_{17}Fe_{74.5}B_{8.5}$, and $Nd_{18}Fe_{73}B_9$ were undercooled and solidified in an 8 m drop tube filled with helium. The microstructure of the received particles was investigated by means of scanning electron microscopy and powder X-ray diffractometry. It was found that in each alloy composition, in excess of 71% of the particle population shows a microstructure comprising primary $Nd_2Fe_{17}B_x$ dendrites plus interdendritic $Nd_2Fe_{14}B$ grains plus intergranular $Nd_{1.1}Fe_4B_4$ and Nd-rich grains, where the metastable $Nd_2Fe_{17}B_x$ dendrites are partially or completely decomposed into a mixture of α-Fe plus $Nd_2Fe_{14}B$ depending on particle size. There is often a certain amount of $Nd_2Fe_{14}B$ dendrites in these particles, resulting in a dual microstructure. On the other hand, the rest of the particle population shows a microstructure consisting of primary $Nd_2Fe_{14}B$ grains, either columnar or dendritic, plus intergranular $Nd_{1.1}Fe_4B_4$ and Nd-rich phase grains. Additionally, a tiny amount of α-Fe dendrites is formed in some of the particles independent of the type of the microstructure. They are exclusively distributed near the particle surface, and are surrounded either by $Nd_2Fe_{14}B$ grains or by $Nd_2Fe_{17}B_x$ grains in individual particles.

Keywords: Metals; Liquid quenching; Scanning electron microscopy; X-ray diffraction analysis

1. Introduction

Liquid undercooling often leads to metastable solidification reactions such as formation of metastable phases in preference to the equilibrium one [1]. Previous work [2] has shown that a metastable compound, $Nd_2Fe_{17}B_x$ ($x \sim 1$), will be primarily crystallized in electromagnetically levitated Nd–Fe–B samples of non-peritectic chemical compositions, provided a critical bulk undercooling is exceeded. The grains of $Nd_2Fe_{17}B_x$, however, are decomposed into an intimate mixture of α-Fe plus $Nd_2Fe_{14}B$ because of slow cooling rates during solidification. In addition, a few α-Fe dendrites have been observed in some of the samples. In terms of the dendritic growth morphology, they have been assumed to transform from high temperature γ-Fe dendrites. The extended formation of primary γ-Fe, followed by peritectic formation of a metastable χ-phase, into non-peritectic Nd–Fe–B compositions has been reported by Schneider et al. in their early work for construction of the ternary Nd–Fe–B alloy phase diagram [3]. Because of similar chemical compositions, the χ-phase has been assumed identical to $Nd_2Fe_{17}B_x$ [4]. In the levitated samples, however, there is no evidence for peritectic formation of the metastable $Nd_2Fe_{17}B_x$ grains around the α-Fe dendrites, thus showing a disagreement with the result of those researchers. In present work, gas-atomized Nd–Fe–B melt droplets of three non-peritectic chemical compositions were undercooled and solidified using the drop tube technique in order to understand this discrepancy.

The drop tube technique has at least three advantages over the electromagnetic levitation technique. First, it allows undercooling and solidification of numerous samples in one

* Corresponding author. Present address: Northeastern University, P.O. Box 314, 3–11 Wenhua Road, Shenyang 110004, China. Tel.: +86-24-8368-1915; fax: +86-24-8368-1758.
E-mail address: jgao@mail.neu.edu.cn (J. Gao).

0925-8388/$ – see front matter © 2004 Elsevier B.V. All rights reserved.
doi:10.1016/j.jallcom.2004.07.027

experiment, thus enabling investigations of solidification statistics of samples of different sizes. Secondly, it allows cooling of the samples at a rate on the order of 10^2 to 10^4 K/s depending on the sample size [5], which is at least by one order higher than that of the levitated samples. Such a high cooling rate reduces temperature rise during recalescence, and hence, helps to preserve initially solidified microstructure down to room temperature. Thirdly, it achieves undercooling of melt droplets under a higher gas pressure, thus avoiding any changes in sample composition associated with the evaporation of elemental Nd during levitation [2]. Because of these advantages, drop tube experiments were expected to shed more light into the metastable solidification behavior of non-peritectic Nd–Fe–B compositions.

2. Experimental

Alloys with atomic composition of $Nd_{16}Fe_{76}B_8$, $Nd_{17}Fe_{74.5}B_{8.5}$, and $Nd_{18}Fe_{73}B_9$ were prepared by arc-melting high purity elemental materials (99.9% purity or better) under the protection of an argon atmosphere. In order to compensate for mass loss during melting, an extra mass of 0.1% was added both for neodymium and for boron. An alloy of 1 g was placed in a quartz tube with an orifice of 0.5 mm opened at the bottom. The quartz tube was positioned in a copper coil fixed at the top of an 8 m drop tube [6]. After evacuation to a vacuum pressure in the order of 10^{-4} Pa, the drop tube was backfilled with pure helium (99.999% purity) to a pressure of about 50 kPa. The alloy was inductively melted, and heated to a temperature of 100–200 K above its liquidus. By introduction of an argon gas flow into the quartz tube, the melt was ejected through the nozzle, and atomized into droplets of diameter ranging from 0.1 to 2.0 mm. The droplets were containerlessly undercooled and solidified during their free fall in the drop tube. The solidified particles were collected at the bottom of the drop tube, and sieved into several group sizes. The particles of each group size were mounted in an epoxy resin, ground and polished to a finish of 0.25 μm. Then, their microstructure was examined using a high resolution LEO 1530VP scanning electron microscope (SEM) under back-scattering conditions. Elemental concentrations, except for boron, of phase constituents were analyzed using an energy dispersive X-ray micro-analyzer (EDX) fitted to the SEM. Powder X-ray diffraction analysis with Fe Kα radiation (λ = 0.1937 nm) was carried out on the particles extracted from the epoxy resin or obtained under identical experimental conditions.

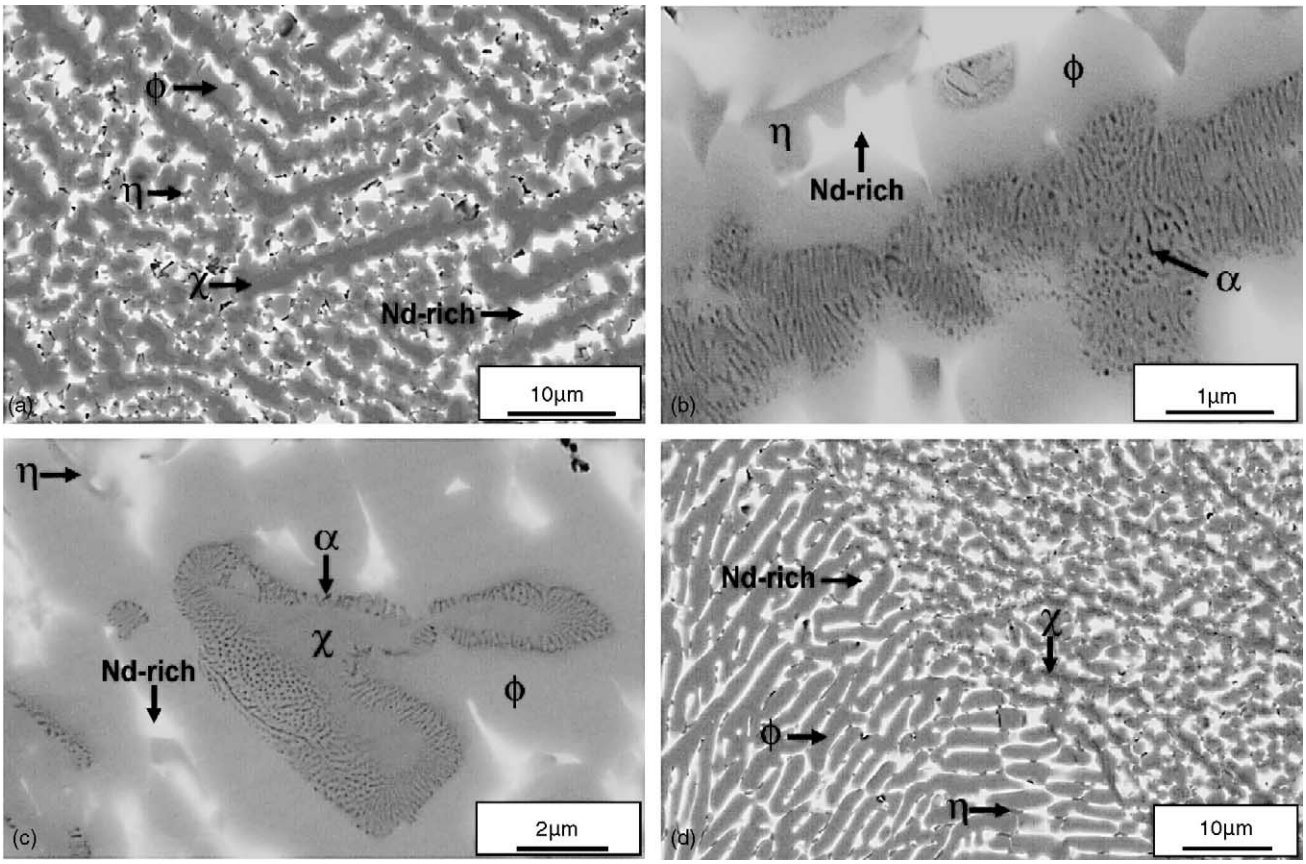

Fig. 1. Back-scattered SEM micrographs illustrating the first type of microstructure, where χ = $Nd_2Fe_{17}B_x$, ϕ = $Nd_2Fe_{14}B$, η = $Nd_{1.1}Fe_4B_4$, α = bcc Fe. (a) Primary χ dendrites; (b) complete and (c) partial decomposition of χ into α plus ϕ; and (d) local ϕ dendrites.

3. Results

Two types of microstructure were observed in the particles of all three compositions. As illustrated in Fig. 1a, the first type of microstructure comprises primary $Nd_2Fe_{17}B_x$ dendrites plus peritectic $Nd_2Fe_{14}B$ grains plus intergranular $Nd_{1.1}Fe_4B_4$ and Nd-rich grains, where the metastable $Nd_2Fe_{17}B_x$ dendrites have been subjected to partial or complete solid-state decomposition depending on particle size. In large particles, the $Nd_2Fe_{17}B_x$ dendrites are completely decomposed into a mixture of α-Fe plus $Nd_2Fe_{14}B$, as shown in Fig. 1b. In small particles, however, the decomposition is not completed yet. As shown in Fig. 1c, there is a remainder within the original dendrites, particularly at the dendritic core, suggesting that the decomposition starts at the dendritic periphery and progresses inwards. The EDX analysis shows no substantial differences of Nd and Fe concentrations between the decomposed mixture and the remainder. Meanwhile, the high fraction of $Nd_2Fe_{14}B$ in the decomposed mixture implies that the x in the chemical formula of $Nd_2Fe_{17}B_x$ is close to 1, though boron concentrations were not analyzed by EDX. There often exists a considerable amount of $Nd_2Fe_{14}B$ dendrites in the particles showing the first type of microstructure. As illustrated in Fig. 1d, the microstructure of the particles actually becomes dual, where there is a sharp interface dividing the microstructure into two distinct zones. A close examination shows that the $Nd_2Fe_{14}B$ dendrites near the interface are stemmed from neighboring peritectic $Nd_2Fe_{14}B$ grains, whereas those far away from the interface are precipitated directly from the liquid, indicative of a transition of the solidification pathway from primary $Nd_2Fe_{17}B_x$ formation to primary $Nd_2Fe_{14}B$ formation. The second type of microstructure is simple compared with the first type. It consists of primary $Nd_2Fe_{14}B$ grains plus intergranular $Nd_{1.1}Fe_4B_4$ and Nd-rich grains. As shown in Fig. 2, the $Nd_2Fe_{14}B$ grains exhibit two different morphologies, columnar and dendritic. In addition, a few α-Fe dendrites were observed in some of the gas-atomized particles independent of the type of the microstructure. As shown in Fig. 3, they are exclusively distributed near the particle surface, and exhibit a peritectic phase relation either with $Nd_2Fe_{14}B$ grains or with $Nd_2Fe_{17}B_x$ grains in individual particles. Similar to those primary ones shown in Fig. 1, peritectic $Nd_2Fe_{17}B_x$ grains are partially or completely decomposed into a mixture of α-Fe plus $Nd_2Fe_{14}B$ depending on particle size.

The two types of microstructure were investigated as a function of particle size and alloy composition. The results were shown in Fig. 4, where the normalized particle population (NPP) of each type of microstructure is plotted against particle size. It is evident that the two types of microstructure occur in all particle sizes, and that neither of them shows a strong particle-size dependence. Within individual size groups, the NPP of the first type of microstructure exceeds 54%, 81%, and 71% in composition $Nd_{16}Fe_{76}B_8$, $Nd_{17}Fe_{74.5}B_{8.5}$, and $Nd_{18}Fe_{73}B_9$, respectively. On the other hand, the total particle population of the first type of microstructure is even higher, reaching 71%, 86%, and 88%, respectively. Such high NPP values demonstrate that the first type of microstructure is more popular than the second type. Note that the NPP of the first type of microstructure is lower in composition $Nd_{16}Fe_{76}B_8$ than in the other two compositions. This might result from a statistical deviation, for the total particle population of composition $Nd_{16}Fe_{76}B_8$, 107, is much smaller than that of the other two compositions, 454 and 416. By comparing the results of the other two compositions, one cannot ascertain that either type of microstructure has a strong alloy composition dependence.

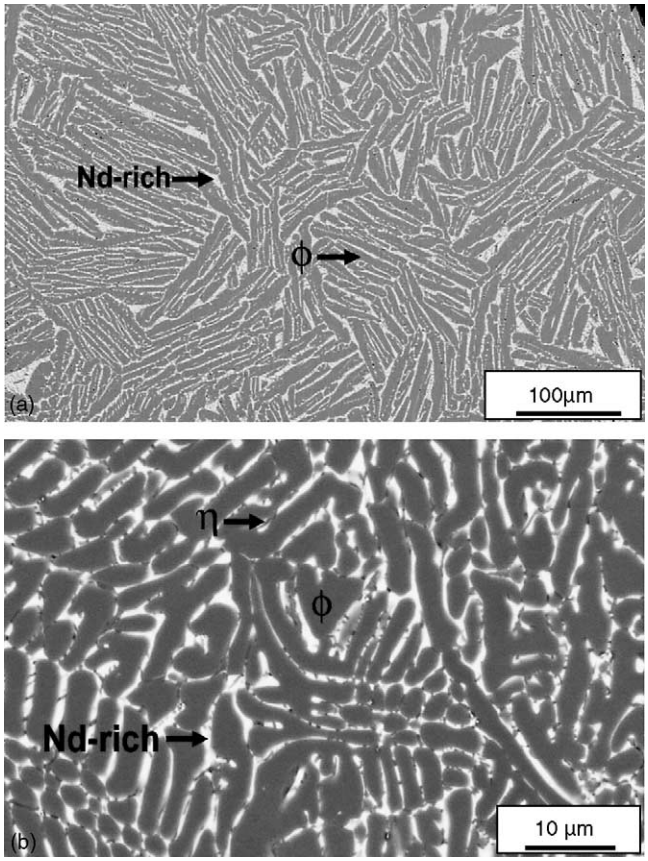

Fig. 2. Back-scattered SEM micrographs illustrating the second type of microstructure, where ϕ = $Nd_2Fe_{14}B$ and η = $Nd_{1.1}Fe_4B_4$. (a) Columnar and (b) dendritic ϕ grains.

The results of powder X-ray diffraction analysis are presented in Fig. 5, showing the same phase constituents, ϕ-$Nd_2Fe_{14}B$, η-$Nd_{1.1}Fe_4B_4$, Nd-rich phase, α-Fe, for the particles of different sizes and alloy compositions. Note that the intensity of the diffraction peaks of the α-phase is very weak, implying that its volume fraction is limited. Such a result agrees well with the SEM investigations. The missing of the diffraction peaks from the metastable $Nd_2Fe_{17}B_x$ was attributed to two factors. One is that the dendrites of $Nd_2Fe_{17}B_x$ are partially or completely decomposed in the particles, and another is that the particles were subjected to a mass loss during grinding and polishing, thus having a further

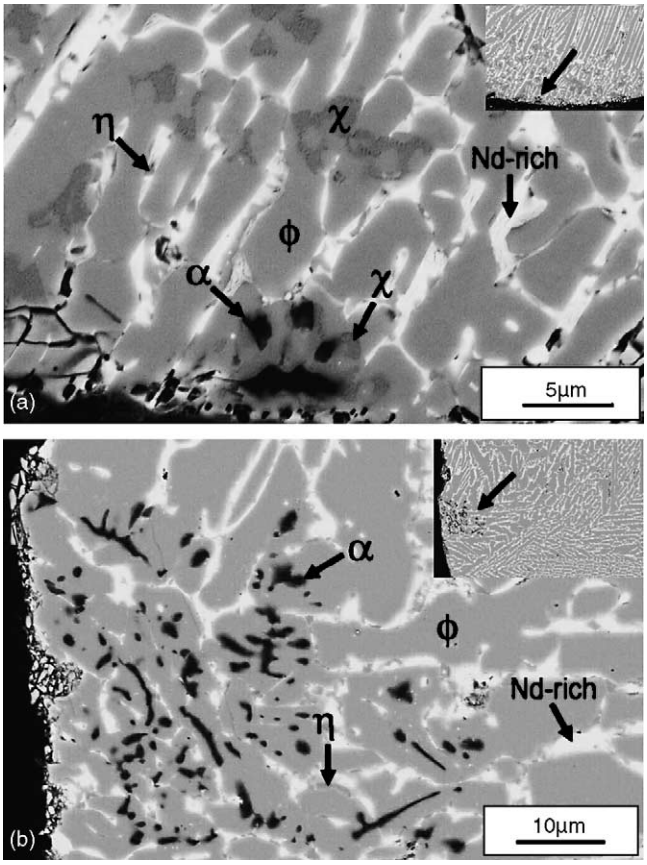

Fig. 3. Back-scattered SEM micrographs illustrating α-Fe dendrites near the particle surface, where α = bcc Fe, ϕ = $Nd_2Fe_{14}B$, χ = $Nd_2Fe_{17}B_x$, η = $Nd_{1.1}Fe_4B_4$. The insets show the microstructure in a larger view. (a) α dendrites plus peritectic χ grains and (b) α dendrites plus peritectic ϕ grains.

reduced amount of $Nd_2Fe_{17}B_x$ dendrites. The second factor is proven more critical because few diffraction peaks from $Nd_2Fe_{17}B_x$ were detected for small-sized $Nd_{16}Fe_{76}B_8$ alloy particles, which were prepared under identical experimental conditions but not subjected to grinding and polishing. As shown in Fig. 6, two additional diffraction peaks appear around the (4 1 0) peak of $Nd_2Fe_{14}B$ in the diffraction pattern of the size group 0.34–0.63 mm, looking like two shoulders. By reference to previous results [7], they were indexed to the (0 0 2) diffraction and to (1 1 1) diffraction of the hexagonal lattice of $Nd_2Fe_{17}B_x$, respectively. Similar results were obtained for the other two compositions.

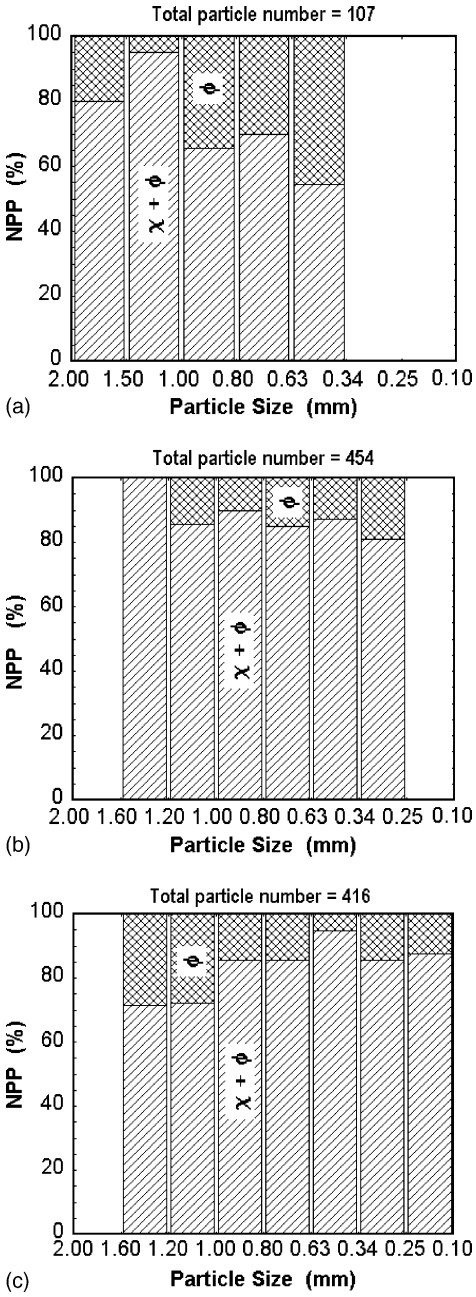

Fig. 4. Normalized particle population (NPP) of the two types of microstructure vs. particle size in different alloy compositions, where shadowed columns are for the first type of microstructure, and gridded columns for the second type of microstructure. Composition: (a) $Nd_{16}Fe_{76}B_8$; (b) $Nd_{17}Fe_{74.5}B_{8.5}$; and (c) $Nd_{18}Fe_{73}B_9$.

4. Discussion

The two types of microstructure of the gas-atomized particles are generally similar to those of levitated bulk samples of the same alloy compositions [2]. For this reason, the first type of microstructure can be related to a large droplet undercooling, whereas the second type to a small droplet undercooling. The more popular formation of the first type of microstructure implies that the majority of the atomized particles has attained a significant liquid undercooling prior to solidification. With respect to the levitated samples, grain sizes of the present particles are reduced, and the solid-state decomposition of the metastable $Nd_2Fe_{17}B_x$ is partially inhibited, particularly in the particles of smaller sizes. These two changes can reasonably be related to higher cooling rates of the gas-atomized particles. In addition, the present results show that the minor α-Fe dendrites are surrounded either by peritectic $Nd_2Fe_{14}B$ grains or by peritectic $Nd_2Fe_{17}B_x$ grains in

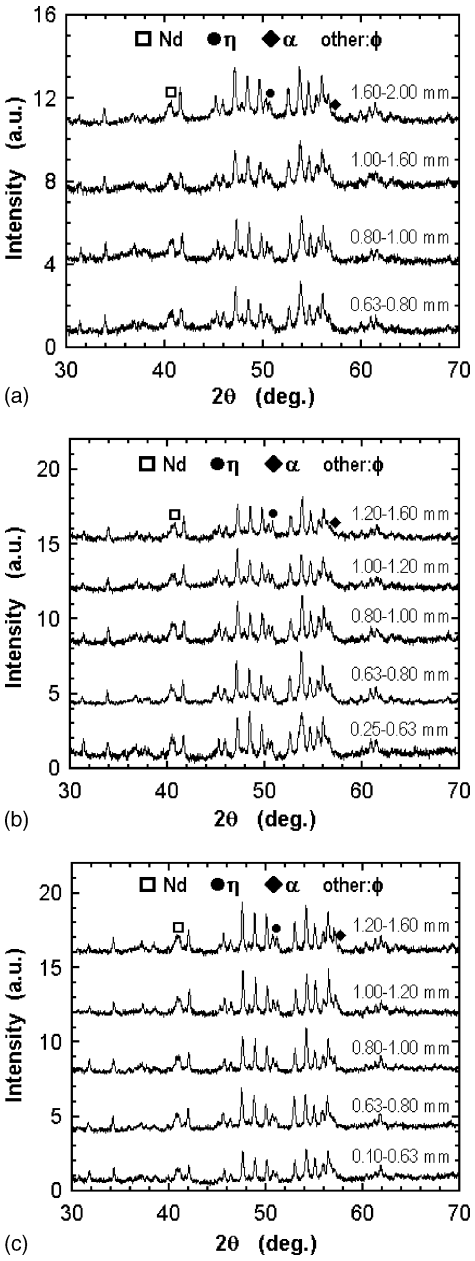

Fig. 5. Powder X-ray diffraction patterns of the particles of different alloy compositions, where ϕ = $Nd_2Fe_{14}B$, η = $Nd_{1.1}Fe_4B_4$, Nd = Nd-rich, α = bcc Fe. Composition: (a) $Nd_{16}Fe_{76}B_8$; (b) $Nd_{17}Fe_{74.5}B_{8.5}$; and (c) $Nd_{18}Fe_{73}B_9$.

individual particles. Although the conditions under which the two species of peritectic grains occur have not been determined yet, such a finding conciliates the disagreement between the early work of Schneider et al. [3] and our previous work [2] regarding γ-Fe solidification, which is implied by the occurrence of the low temperature α-Fe dendrites. In previous work [2], γ-Fe solidification has been explained in two different ways. Based on a calculated peritectic liquid composition of $Nd_{17.9}Fe_{73.2}B_{8.9}$ for the ternary Nd–Fe–B alloy system [8], the first explanation views γ-Fe as a near-equilibrium solidification product within remaining liquid after a strong recalescence event (namely, both primary $Nd_2Fe_{14}B$ and primary $Nd_2Fe_{17}B_x$ are metastable with respect to the equilibrium primary γ-Fe). While keeping the peritectic liquid composition of $Nd_{15.7}Fe_{76.45}B_{7.85}$ as proposed by Schneider et al. [3], the second explanation views γ-Fe as a metastable and primary phase, the nucleation of which can occur concurrently with that of the metastable $Nd_2Fe_{17}B_x$. According to the present results, the first explanation can be ruled out. As seen in the insets of Fig. 3, the minor α-Fe dendrites grow along the same direction as that of primary $Nd_2Fe_{14}B$ dendrites or of primary $Nd_2Fe_{17}B_x$ dendrites nearby, thus implying that their high temperature ancestors, γ-Fe dendrites, are unlikely to be a post-recalescence solidification product. On the other hand, the second explanation is well supported by the present results directly. It is evident in the micrograph of Fig. 3a that many $Nd_2Fe_{17}B_x$ dendrites are nucleated independently close to the particle surface, though peritectic grains of the same species in a very limited amount are nucleated around the α-Fe dendrites. More clear evidence was shown by the micrograph of Fig. 7, where one α-Fe dendrite and one $Nd_2Fe_{17}B_x$ dendrite are formed close to each other,

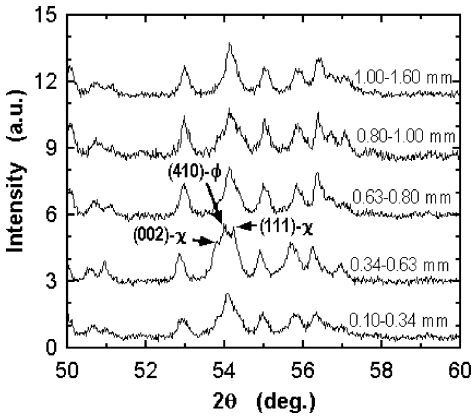

Fig. 6. Powder X-ray diffraction patterns of unpolished $Nd_{16}Fe_{76}B_8$ alloy particles, where χ = $Nd_2Fe_{17}B_x$ and ϕ =$Nd_2Fe_{14}B$.

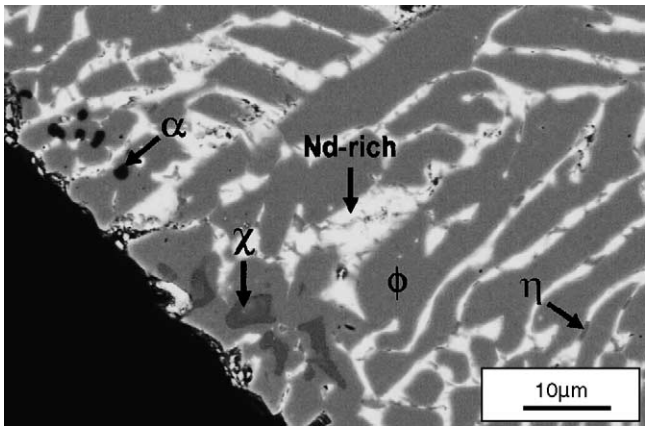

Fig. 7. Back-scattered SEM micrograph showing individual α-Fe and $Nd_2Fe_{17}B_x$ dendrites in one particle of composition $Nd_{17}Fe_{74.5}B_{8.5}$, where α = bcc Fe, χ = $Nd_2Fe_{17}B_x$, ϕ = $Nd_2Fe_{14}B$. Note that there are no peritectic χ grains around the α dendrite.

but there are no peritectic $Nd_2Fe_{17}B_x$ grains around the α-Fe dendrite. Such a microstructure, though observed only in a few particles, clearly demonstrates that under certain conditions, the high temperature γ-Fe phase and $Nd_2Fe_{17}B_x$ can be simultaneously nucleated from undercooled liquids, i.e. both of them are primary phases. It should be pointed out that a solidified microstructure is determined not only by nucleation, but also by growth, of crystalline phases. Due to the fact that crystal growth in undercooled melts is strongly affected by solute rejection in front of the liquid/crystal interface [9], the limited amount of the α-Fe dendrites in the final microstructure can be attributed to more sluggish growth kinetics of γ-Fe dendrites than that of $Nd_2Fe_{17}B_x$ dendrites during solidification.

In summary, the present results not only conciliate the disagreement between the work of Schneider et al. and the previous work with respect to γ-Fe solidification, but also verify the simultaneous and independent nucleation of the metastable γ-Fe and $Nd_2Fe_{17}B_x$ in non-peritectic Nd–Fe–B compositions.

5. Conclusions

Two types of microstructure have been observed in gas-atomized particles of three non-peritectic Nd–Fe–B compositions. One is featured by primary formation of the metastable $Nd_2Fe_{17}B_x$ dendrites, whereas another is featured by predominant primary formation of the stable $Nd_2Fe_{14}B$ grains. They are generally similar to those observed in levitated bulk samples of the same alloy compositions, except for reduced grain sizes and partial suppression of the solid-state decomposition of $Nd_2Fe_{17}B_x$. Additionally, a tiny amount of α-Fe dendrites has been observed in some of the particles independent of the type of the microstructure. They are exclusively distributed near the particle surface, and are surrounded either by peritectic $Nd_2Fe_{14}B$ grains or by peritectic $Nd_2Fe_{17}B_x$ grains in individual particles. Such results not only conciliate the disagreement between the early work of Schneider et al. and the previous work with respect to γ-Fe solidification, but also verify the simultaneous and independent nucleation of γ-Fe and $Nd_2Fe_{17}B_x$ in non-peritectic Nd–Fe–B compositions.

Acknowledgements

This work is financially supported by DLR-Bonn under contract no. 50WM9930. The authors thank Dr. H. Bach of Ruhr-University of Bochum, for his continuous support. One of the authors, J. Gao, is grateful to the Alexander von Humboldt Foundation for a long-term research fellowship.

References

[1] D.M. Herlach, Mater. Sci. Eng. A226–228 (1997) 348–356.
[2] J. Gao, T. Volkmann, D.M. Herlach, J. Alloys Compd. 350 (2003) 344–350.
[3] G. Schneider, E.Th. Henig, G. Petzow, H.H. Stademaier, Z. Metallkd. 77 (1986) 755–761.
[4] J. Gao, Th. Volkmann, D.M. Herlach, J. Alloys Compd. 308 (2000) 296–300.
[5] J. Fransaer, private communication.
[6] F. Gillessen, D.M. Herlach, Mater. Sci. Eng. 97 (1988) 147–151.
[7] J. Gao, T. Volkmann, S. Roth, W. Löser, D.M. Herlach, J. Magn. Magn. Mater. 234 (2001) 313–319.
[8] B. Hallemans, P. Wollants, J.R. Roos, J. Phase Equilib. 16 (1995) 137–149 (those researchers gave a non-balanced composition of the peritectic liquid in the ternary Nd–Fe–B alloy system. Because they stated that it has an Fe concentration of 73.2 at.%, we took the 2/3 of the balance, 17.9 at.%, for elemental Nd and the 1/3 of the balance, 8.9 at.%, for elemental B).
[9] K. Eckler, R.F. Cochrane, D.M. Herlach, B. Feuerbacher, Mater. Sci. Eng. A133 (1991) 702–705.